REFERENCES

[1] T. Yoneyama and S Nishida, "Nonradiative dielectric waveguide for millimeter-wave integrated circuits," *IEEE Trans. Microwave Theory Tech.*, vol. MTT-29, pp. 1188–1192, Nov. 1981.

[2] T. Yoneyama, N. Tozawa, and S. Nishida, "Coupling characteristics of nonradiative dielectric waveguides," *IEEE Trans. Microwave Theory Tech.*, vol. MTT-31, Aug. 1983.

[3] T. Yoneyama, F. Kuroki, and S. Nishida, "Design of nonradiative dielectric waveguide filters," *IEEE Trans. Microwave Theory Tech.*, vol. MTT-32, Dec. 1984.

[4] J. A. Paul and P. C. H. Yen, "Millimeter-wave passive components and six-port network analyzer in dielectric waveguide," *IEEE Trans. Microwave Theory Tech.*, vol. MTT-29, pp. 948–953, Sept. 1981.

[5] K. Ogusu, "Dielectric waveguide corner and power divider with a metallic reflector," *IEEE Trans. Microwave Theory Tech.*, vol. MTT-32, pp. 113–116, Jan. 1984.

A Novel Method for the Analysis of Microwave Two-Port Active Mixers

J. DREIFUSS, A. MADJAR, AND A. BAR-LEV

Abstract—**An analysis method for a microwave mixer, based on an active nonlinear device, is developed. The method is a two-port extension of Kerr's work on a one-port (diode)-type mixer and utilizes the harmonic balance approach for the large-signal analysis portion. It results in a relatively fast and efficient program, the use of which is demonstrated by simulating the operation of a mixer based on a NEC MESFET for a range of local oscillator available power and frequency conditions.**

I. INTRODUCTION

Microwave mixers have normally been based on Schottky-barrier diodes. Lately, major advances in GaAs technology have led to a new type of an active microwave mixer based on a two-port device, the MESFET, which is likely to find wide use in the future [1]–[5]. The advantages of such a mixer are a) conversion gain, b) self-oscillation option, c) natural isolation between device terminals (makes filters unnecessary), and d) compatibility with GaAs monolithic technology.

While experimental data on MESFET mixers is available, little has been published so far on theoretical methods for two-port mixer analysis. Preliminary investigation of this topic was performed by Pucel *et al.* [1], Ntake [2], Harrop [3], and Kurita and Morita [4]. A more systematic approach by Mass [5] uses Kerr's single-port method [6], [7], originally applied to diode mixers, for each of the nonlinear elements in the FET equivalent circuit.

This paper proposes a new approach to the general analysis of two-port mixers which is a true two-port extension of Kerr's method. The active device is represented by a mathematical two-port model and not by a specific equivalent circuit. This simplifies the adaptation of the analysis program to other devices: one needs only change the subroutine that calculates the two-port parameters. The method is quite general and any type of mixer can be analyzed (ordinary, subharmonic, high IF, etc.).

Moreover, as signal analysis is performed by the harmonic balance method, which is very fast and accurate, any number of the LO harmonics and small signals can be considered to improve accuracy.

Manuscript received February 7, 1985; revised June 6, 1985.

J. Dreifuss and A. Madjar are with the Israeli Ministry of Defense, Armament Development Authority, P.O. Box 2250, Haifa 31021, Israel.

A. Bar-Lev is with the Technion-Israel Institute of Technology, Department of Electrical Engineering, Haifa, Israel.

II. OUTLINE OF THE MIXER ANALYSIS METHOD

As in Kerr's work [6], [7], the analysis method is composed of large- and small-signal analyses parts. The first is performed on the nonlinear circuit excited by the large LO signal alone. As the other signals present are very small, it is assumed that they do not affect the device parameters and all the pumping effects are due to the LO signal only. From the voltage and current waveforms obtained, conductance-like and capacitance-like waveforms are derived which are then used in the small-signal analysis to characterize the device as a linear time varying network. The relations between the small-signal voltages and currents of the various frequencies are obtained from the network in the form of an admittance matrix whose elements are 2×2 submatrices. Combining this matrix with the source and load constraints at each frequency makes possible the calculation of the mixer performance parameters, such as conversion gain and input and output impedances. The two parts of the analysis are detailed below.

III. LARGE-SIGNAL ANALYSIS

The large-signal analysis step uses the standard two-port representation for the device. Six coefficients which are nonlinear functions of the voltages $V_1(t), V_2(t)$ are used to relate the currents and voltages

$$I_1(t) = I_{\text{con}_1} + (CV)_{11}\frac{dV_1(t)}{dt} + (CV)_{12}\frac{dV_2(t)}{dt} \tag{1}$$

$$I_2(t) = I_{\text{con}_2} + (CV)_{21}\frac{dV_1(t)}{dt} + (CV)_{22}\frac{dV_2(t)}{dt} \tag{2}$$

where

$I_1(t)$ current waveform at port 1

$I_2(t)$ current waveform at port 2

$V_1(t)$ voltage waveform at port 1

$V_2(t)$ voltage waveform at port 2.

A computer model that calculates the six coefficients for a given V_1, V_2 in the case of a MESFET was presented by Madjar and Rosenbaum [8], [9] and later modified by Green *et al.* [10]. This model is used here.

The complete circuit of the MESFET is shown in Fig. 1 in which the box at the center represents the intrinsic FET.

In order to obtain the current and voltage waveforms in the steady state, the harmonic balance method [11] is used because of its efficiency (short computing times). The method divides the network into linear and nonlinear parts and then matches the currents between the two parts at their interface. The voltages at the interface (which are of course the same for the two parts), are used to derive these currents. Treating the interface voltages as variables and the difference in the respective currents at the interface as the function for an optimization routine leads to the correct solution for voltages and currents at the interface nodes. As these quantities are presented by their Fourier series, it is the Fourier coefficients that are the optimization variables. The ZSPOW optimization routine from IMSL (International

0018-9480/85/1100-1241$01.00 ©1985 IEEE

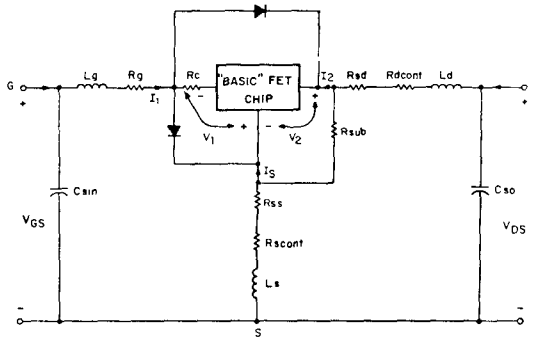

Fig. 1. Complete MESFET circuit model.

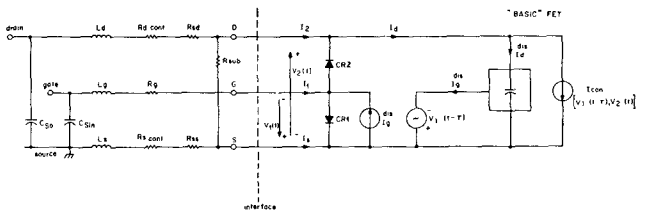

Fig. 2. Complete mixer network for the harmonic balance analysis.

Mathematics & Statistical Library) package was utilized here. The partitioned network for the MESFET mixer, which uses the above mentioned MESFET model is shown in Fig. 2. This network includes the MESFET model [8], [9] as in Fig. 1 with the modification by Green *et al.* [10] (R_c is replaced by a delayed voltage source. τ = channel transit time).

The large-signal analysis yields a set of Fourier coefficients for I_1, I_2, V_1, V_2, from which the waveforms of the six coefficients in (1) and (2) are derived. From these the small-signal conductances, defined as follows, are derived:

$$g_{11} = \frac{\partial I_{\text{con}_1}}{\partial V_1} \qquad g_{12} = \frac{\partial I_{\text{con}_1}}{\partial V_2}$$

$$g_{21} = \frac{\partial I_{\text{con}_2}}{\partial V_1} \qquad g_{22} = \frac{\partial I_{\text{con}_2}}{\partial V_2}. \tag{3}$$

The eight waveforms of the four conductances and four capacitances are therefore expressed as

$$(CV)_{i,j}(t) = \sum_{k=-\infty}^{\infty} C_k^{i,j} \exp(jk\omega_{\text{LO}}t) \quad C_{-K} = C_K^*$$

$$g_{i,j}(t) = \sum_{k=-\infty}^{\infty} G_k^{i,j} \exp(jk\omega_{\text{LO}}t) \quad G_{-K} = G_K^*. \tag{4}$$

IV. Small-Signal Analysis

The small-signal characterization of the device is obtained from (1) and (2)

$$i_1 = g_{11}v_1 + g_{12}v_2 + (CV)_{11}\frac{dv_1}{dt} + (CV)_{12}\frac{dv_2}{dt}$$

$$i_2 = g_{21}v_1 + g_{22}v_2 + (CV)_{21}\frac{dv_1}{dt} + (CV)_{22}\frac{dv_2}{dt}. \tag{5}$$

The Fourier expansions in (4) for the eight coefficients are now substituted in (5).

Following Saleh's work [12], the only small-signal frequencies of interest are

$$\omega_m = \omega_{\text{IF}} + m\omega_{\text{LO}}, \qquad m = 0, \pm 1, \pm 2, \cdots, \pm\infty. \tag{6}$$

One can therefore express the small-signal currents i_1, i_2 and voltages v_1, v_2 in (5) as infinite series composed of only those frequencies, i.e.,

$$i_1(t) = \sum_{m=-\infty}^{\infty} I_m^{(1)} e^{j\omega_m t}, \qquad I_{-m}^{(1)} = I_m^{(1)*}. \tag{7}$$

Using this, (5) can be put in the form of an admittance matrix

$$\begin{bmatrix} \cdot \\ \cdot \\ \bar{I}_1 \\ \bar{I}_0 \\ \bar{I}_{-1} \\ \cdot \\ \cdot \end{bmatrix} = \begin{bmatrix} \cdot & \cdot & \cdot & \cdot & \cdot & \cdot \\ \cdot & \cdot & \cdot & \cdot & \cdot & \cdot \\ \cdot & \bar{Y}_{1,1} & \bar{Y}_{1,0} & \bar{Y}_{1,-1} & \cdot & \\ \cdot & \bar{Y}_{0,1} & \bar{Y}_{0,0} & \bar{Y}_{0,-1} & \cdot & \\ \cdot & \bar{Y}_{-1,1} & \bar{Y}_{-1,0} & \bar{Y}_{-1,-1} & \cdot & \\ \cdot & \cdot & \cdot & \cdot & \cdot & \\ \cdot & \cdot & \cdot & \cdot & \cdot & \end{bmatrix} \begin{bmatrix} \cdot \\ \cdot \\ \bar{V}_1 \\ \bar{V}_0 \\ \bar{V}_{-1} \\ \cdot \\ \cdot \end{bmatrix} \tag{8}$$

where

$$\bar{I}_k = \begin{pmatrix} i_1 \\ i_2 \end{pmatrix}_k, \bar{V}_l = \begin{pmatrix} v_1 \\ v_2 \end{pmatrix}_l, \bar{Y}_{k,l} = \begin{pmatrix} y_{11} & y_{12} \\ y_{21} & y_{22} \end{pmatrix}$$

and

$$y_{i,j|k,l} = G_{k-l}^{i,j} + j\omega_l C_{k-l}^{i,j}, \quad i,j = 1,2. \tag{9}$$

The infinite set of equations (8) relates all the small-signal voltages and currents at all the relevant frequencies ω_m given by (6) and is similar to Kerr's set of equations except that here the elements of the admittance matrix are 2×2 submatrices. Thus, $\bar{Y}_{k,l}$ is the two-port matrix relating currents i_1, i_2 at ω_k to voltages v_1, v_2 at ω_l.

To solve the network under consideration, the source and load admittances at all the relevant frequencies must be added as external constraints. In the practical case, only a finite number of frequencies ω_m is used in the calculations, i.e., the Y matrix is truncated, with some sacrifice in accuracy.

The mixer conversion gain between frequencies ω_k at port 1 and ω_l at port 2 and its input and output admittances are given by

$$(\text{GAIN})_{k,l} = 4|Z_{21}|_{k,l}^2 \cdot \text{Re}\left[Y_{G_k}\right] \cdot \text{Re}\left[Y_{D_l}\right] \tag{10}$$

$$Y_{\text{in}_k} = (Z_{11})_{k,k}^{-1} - Y_{G_k} \tag{11}$$

which is the input admittance at ω_k in the gate

$$Y_{\text{out}_k} = (Z_{22})_{k,k}^{-1} - Y_{D_k} \tag{12}$$

which is the output admittance at ω_k in the drain

where Y_{G_K} is the generator admittance in the gate at ω_k and Y_{D_l} is the load admittance in the drain at ω_l.

The Z matrix appearing in (10)–(12) is the inverse of the Y matrix of the complete network. This includes the device itself, its parasitics as shown in Fig. 1, the load admittance at the drain, and the source admittance at the gate for the various Saleh frequencies ω_m. The matrix of the complete network is derived from that of the intrinsic device, (8), by adding to it the linear part of the external network. First, the parallel connected elements are added to the main diagonal submatrices of Y, which is then inverted to obtain a Z matrix. The series-connected elements are then added to the main diagonal submatrices of Z. This procedure must be repeated until all the elements of the external network are included. Note that linear elements appear

TABLE I
DEVICE PARAMETERS FOR NE 720

EPI layer thickness = 0.135μm
Doping level = 3×10^{17} cm^{-3}
Gate length = 1μm Gate width = 400μm
Rss = Rsd = 0.965Ω Rg = 2Ω
Rscont = Rdcont = 1Ω Rsub = 500Ω
Lg = 0.35 nHy Ls = 0.17 nHy Ld = 0.4nHy
Csin = Cso = 0.15PF

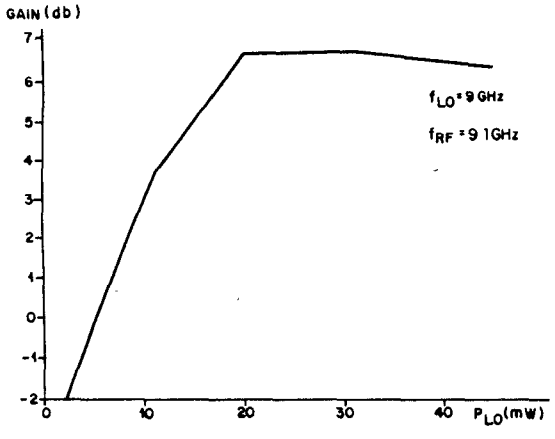

Fig. 3. Gain of the FET mixer versus LO available power

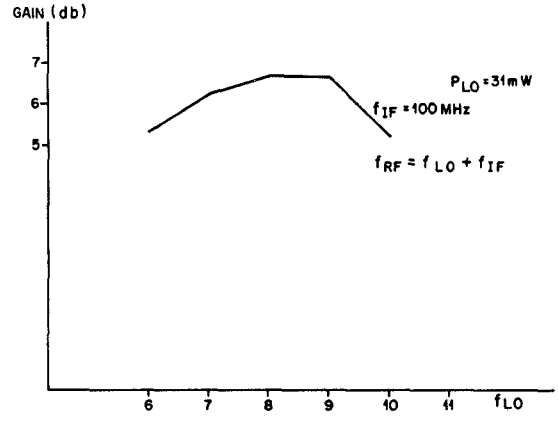

Fig. 4. Gain of the FET mixer versus LO frequency.

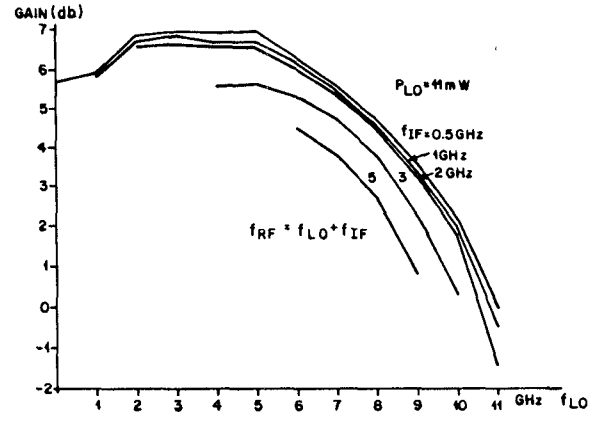

Fig. 5. Gain of the FET mixer versus LO and IF frequencies.

only in main diagonal submatrices as they cannot interrelate currents and voltages at different frequencies.

Equation (10) for the mixer gain is quite general. For normal mixers, $k = 1$ for the upper sideband (or $k = -1$ for the lower sideband) and $l = 0$. For the subharmonic mixer, $|k| > 1$ and $l = 0$. For upconversion, $k = 0$ and $l = 1$ or -1. For harmonic upconverters, $k = 0$ and $|l| > 1$.

V. SIMULATION EXAMPLE

The analysis method outlined above was applied to an FET mixer operated at various frequencies and power conditions and in which the parameters of the NEC NE720 MESFET device were used (see Table I). No attempt was made to design an optimized mixer, as the purpose of the simulation was only to demonstrate the capability and computational efficiency of the proposed method. The simulated network included the device itself, in common source configuration, and 50-Ω constant resistive loads at both gate and drain. The LO and RF signals were injected in the gate and the IF extracted at the drain. The device was operated near pinchoff and $V_{DS} = 2$ V. Fig. 3 shows the mixer conversion gain versus the available power of the LO. As expected, the gain increases with LO power up to about 20 mW and then saturates and remains fairly constant at about 6.5 dB. A typical run of the program used to calculate each data point takes about 30 s on a CDC 6600 computer. The simulations were performed with 8 LO harmonics (18×18 matrix). This was found satisfactory, and no improvement was gained by increasing that number.

Fig. 4 presents the conversion gain versus LO and signal frequencies (fixed IF frequency) for a constant available power of LO. The gain peaks at about 6.7 dB for the LO frequency range of 8 to 9 GHz.

Fig. 5 gives the conversion gain as function of the LO frequency where f_{IF} is taken as a parameter and the available LO power is fixed. Again, there is a range of LO frequencies at which the gain peaks and is higher when the intermediate frequency is lower.

The fast decrease of the gain at the higher frequencies is due mainly to increased VSWR at the LO port, which results in reduced LO power delivered to the FET. Additional conclusions that can be drawn from Fig. 4 are that at high LO power the gain stays high even at 9 or 10 GHz (presumably because at those high-power levels we are still in or near the gain saturation region of Fig. 3 in spite of some LO power reflection). This indicates that a wide-band matching network at the LO port will result in a wide-band FET mixer.

Experimental verification of the proposed theory is performed and will be the topic of a future paper. Some preliminary results have been obtained by operating the NE720 device (mounted in an MIC fixture) as a simple mixer with no matching networks at the operating conditions, as in Fig. 4. A conversion gain of approximately 5 dB was achieved over LO frequencies 4–8 GHz.

VI. CONCLUSION

A new method has been presented for the analysis of microwave two-port active mixers. The new method is a true two-port extension of Kerr's approach to one-port mixers. The large-signal

analysis is performed by the harmonic balance approach, thus yielding an efficient and fast computer analysis program. The usefulness and efficiency of the method is demonstrated by a simulation example of a MESFET mixer.

References

[1] R. A Pucel, D Masse, and R. Bera, "Performance of GaAs MESFET mixers at X-Band," *IEEE Trans. Microwave Theory Tech.*, vol. MTT-24, pp. 351–360, June 1976

[2] P. L Ntake, A computer-aided design of low-noise parametric down converters and GaAs FET mixers for low-cost satellite microwave receivers," Ph.D. dissertation, Carleton Univ., Ottawa, Ont Canada, 1977

[3] P. Harrop, "GaAs FET mixers: Theory and applications," *Acta Electronica* (France), vol. 23, no. 4, pp. 291–297, 1980.

[4] O Kurita and K. Morita, "Microwave MESFET mixers," *IEEE Trans Microwave Theory Tech.*, vol MTT-24, pp. 361–366, June 1976.

[5] S A Mass, "Theory and analysis of GaAs MESFET mixers," *IEEE Trans. Microwave Theory Tech*, MTT-32, pp. 1402–1406, Oct. 1984

[6] P. H. Seigel and A. R Kerr, "A user oriented computer program for the analysis of microwave mixers, and a study of the effects of the series inductance and diode capacitance on the performance of some simple mixers," NASA Goddard for Space Studies, Goddard Space Flight Center NY.

[7] A. R. Kerr, "Noise and loss in balanced and subharmonically pumped mixers: Part I—Theory and Part II—Application," *IEEE Trans. Microwave, Theory Tech.*, vol. MTT-27, pp 938–950, Dec. 1979

[8] A. Madjar and F. J. Rosenbaum, "An ac large signal model for the GaAs MESFET," Department of Electrical Engineering, Washington University, St. Louis, MO, Final Rep. Contract N00014-78-C-0256, Aug 1979

[9] A Madjar and F. J. Rosenbaum, "A practical ac large signal model for GaAs microwave MESFET," in *IEEE MTT-S Symp. Dig.*, 1979.

[10] D. R. Green, Jr., and F. J Rosenbaum, "Performance limits on GaAs FET large and small signal circuits," Tech. Rep NRL-81-1, Department of Electrical Engineering, Washington University, St. Louis, MO, Oct. 1981.

[11] M S. Nakhla and J. Valach, "A piecewise harmonic balance technique for determination of periodic response of nonlinear systems," *IEEE Trans. Circuits Syst.*, vol. CAS-23, pp. 85–91, Feb. 1976.

[12] A. A. M. Saleh, *Theory of Resistive Mixers*. Cambridge, MA., MIT Press, 1971.

Single-Stage GaAs Monolithic Feedback Amplifiers

C. E. WEITZEL, SENIOR MEMBER, IEEE, AND
D. SCHEITLIN, MEMBER, IEEE

Abstract—**A theoretical and experimental comparison is made of the performance of GaAs MESFET's with and without negative feedback. The devices are fabricated using a six-step MMIC process, which utilizes polyimide for low-capacitance crossovers and silicon nitride for MIM capacitors. Typical RF performance is 9-dB gain with noise figure less than 4 dB from 100 MHz to 3 GHz. The greatest bandwidth is achieved by incorporating a $3\frac{1}{2}$ turn, low Q inductor, which is connected in series with the feedback resistor and is wrapped around the perimeter of the chip to conserve die area.**

I. Introduction

Negative feedback has been shown to be a viable technique for making wide-band amplifiers with GaAs MESFET's. Ulrich [1] reported a wide-band, hybrid amplifier with a gain of 6.5 dB from 10 MHz to 6 GHz. The amplifier was built with a GaAs FET with a transconductance of ~ 75 mS. Several GaAs monolithic amplifiers using negative feedback have also been reported. Nishiuma *et al.* [2] reported a single-stage monolithic feedback amplifier with 8–10-dB gain and a 2.2-dB noise figure from 50 to 2000 MHz. Archer *et al.* [3] built a two-stage GaAs monolithic amplifier with 24-dB gain, a 3-dB bandwidth to 930 MHz, and a noise figure of 5 dB. Honjo *et al.* [4] reported a two-stage monolithic amplifier with 16-dB gain from 9 MHz to 3.9 GHz and with less than 3-dB noise figure from 90 MHz to 3.9 GHz. The first three-stage, negative feedback GaAs amplifier was reported to have 28-dB gain from 30 MHz to 1.7 GHz [5]. In all of these amplifiers, the amount of feedback was controlled by a resistor between gate and drain.

Higher frequency performance has been achieved by adding inductive elements to negative feedback amplifiers. A minimum gain of 4 dB up to 14 GHz was achieved with negative feedback amplifiers by adding drain and feedback inductors [6] or distributed circuit elements [7]. Terzian *et al.* [8] used a gate, drain, and feedback inductor and achieved 6-dB gain from 1–7 GHz, but the noise figure > 6.5 dB was high. A gain of 6 dB from 0.6–6 GHz was reported by Rigby *et al.* [9] for a one-stage amplifier, which used five inductive elements in a 2.8 mm$\times$1.8 mm die. After careful and detailed modeling, Pavio *et al.* [10] achieved 8-dB gain from 6 to 18 GHz with a feedback amplifier.

The work reported here was undertaken to theoretically and experimentally determine the performance tradeoffs that can be made by monolithically adding resistive and resistance-inductive feedback between the gate and drain of a GaAs MESFET. The predicted and actual performance of a 1-mm-wide GaAs MESFET was compared with that of a similar FET to which feedback was added. The theoretical and experiment results showed that the bandwidth of a resistive feedback amplifier can be increased from less than 2 GHz to over 3 GHz by adding a single, low Q inductor in series with the feedback resistor.

II. Circuit Modeling

The amplifiers were designed using a small-signal MESFET model and COMPACT,[1] a microwave design program. A 1-mm wide FET was selected so that the amplifier would have sufficient gain once the feedback was added. The small-signal model for a 1000-μm-wide GaAs MESFET is shown in Fig. 1. This model was similar to those found in the literature [11]–[13]. The element values were determined from a review of the literature and proper scaling to the 1000-μm width. The FET model was used to predict the gain and noise figure of the FET from 100 Mz to 5 GHz with feedback resistors of various sizes (Fig. 2). The performance of the 1-mm wide FET with no feedback corresponds to the curve with $R_F = \infty$. The predicted gain of the FET was nearly 16 dB at 100 MHz with no feedback but decreased as R_F was decreased. The Fukui equations and the constants k_1 and k_2 reported by Fukui were used to calculate $NF_{\min}$, Γ_{opt}, and R_N [14], [15]. These three parameters were then used to model the noise performance of the FET with and without feedback. The noise figure of the FET was less than 1 dB at 100 MHz and 2.5 dB with $R_F = 150\ \Omega$. The modeling clearly showed that the addition of a few hundred Ω feedback resistor R_F degraded the FET performance.

The addition of feedback, however, had the beneficial effect of reducing the input impedance of the FET and thereby improving

Manuscript received Feb. 17, 1985; revised May 17, 1985

The authors are with the Semiconductor Research and Development Laboratories, Motorola, Inc., 5005 E McDowell Rd., Phoenix, AZ 85008.

[1] COMPACT Engineering, Palo Alto, CA.

0018-9480/85/1100-1244$01.00 ©1985 IEEE